

高耐用溶鋼用ランスの開発

Development of High Durability Lance for Steel Ladle Treatment

山田啓介*, 笹谷佳寛**, 野村 輝***, 松井俊介****, 筒井康志*****

Keisuke YAMADA*, Yoshihiro SASATANI**, Akira NOMURA***,
Shunsuke MATSUI**** and Yasushi TSUTSUI*****

1 緒言

日本製鉄(株)関西製鉄所和歌山地区ステンレス製鋼工場では、溶鋼の温度と成分調整、均一化のために鍋内に上吹き溶鋼用ランス（これ以降はLTランスと記載）を挿入し、ガス吹きを実施している。LTランスは溶融スラグと接し、かつArガスやN₂ガスによる攪拌のために高い耐スポーリング性と耐食性が要求される。

2018年当時に適用していたLTランスの平均寿命は11.1chと短く、ランス交換の作業負荷や耐火物のコスト増が問題となっていた。ランス交換の要因としては、スラグライン部の溶損や下端部の亀裂拡大および剥離であった。特に、下端部の亀裂発生は短寿命（早期交換）の主要因であり、対策が必要であった。

今回、LTランス短寿命の主要因であった下端部亀裂の発生を抑制できる耐火物材質について検討した結果、耐用寿命を60%延ばす改善ができた。その取り組みについて報告する。

2 LTランスの実機使用状況

2・1 材質及び交換理由

従来より適用しているLTランス用耐火物の材質はAl₂O₃-MgO系キャストブルであり、その構成成分を表1に示す。2017～2018年における当社製LTランス交換要因の内訳は図1に示すように、スラグライン部の損耗と亀裂（縦亀裂とリング亀裂）の発生および拡大に関するものが60%以上を占めていた。よって、ランスの耐用向上には、耐火物の亀裂発生対策が必要であった。なお、2018年のLTランス平均寿命は前述のように11.1ch、そして平均累積処理時間は88minであった。

1 Introduction

In order to adjust temperature, composition and uniformity of molten steel in the ladle, the top blowing lance (LT lance) inserts and blows gas into the molten steel in the stainless steel plant of NIPPON STEEL CORPORATION Kansai Works Wakayama Area. The LT lance is in contact with molten slag covering the steel, which is stirred by Ar or N₂ gas blowing, so high spalling and corrosion resistance are required.

Since the average life of the LT lance applied in 2018 was as short as 11.1ch, the increased work load and material cost for the exchange of the lance became problem to be solved. As the major reasons for exchange of the LT lance, corrosion at the slag line, the crack extension and peeling of the tip part were raised. Among them longitudinal crack occurred in the tip part was reason determining for the short life (early exchange), and the effective countermeasure was needed keenly.

Refractory material for use in the LT lance was examined in the present work to decrease crack occurring in the tip part shorting the life of LT lance. As the result, improvement with 60% increase in durability of the LT lance was achieved.

2 Review of LT lance in actual operation

2・1 Material and the reason for the exchange

We use Al₂O₃-MgO castable to the LT lance, and the composition of it is shown in **Table 1**. The reasons for exchange of the LT lance at the years of 2017 and 2018 are shown in **Fig. 1**. The main exchange reason were corrosion of slag line, generation and extension of cracks (in either case of longitudinal and circular), sharing more than 60% with the generation and extension of cracks. Therefore, to improve the life of the LT lance, it is important to prevent occurrence of cracking from the refractories used in the lance. According to the record in 2018, the average life of the LT lance was 11.1ch as described previously and the average cumulative immersion time to exchange was 88min.

* 技術研究所 共通基盤研究センター アシスタントマネージャー Assistant Manager, Fundamental Research Center, Technical Research Labs.
** 不定形製造事業部 不定形技術部 マネージャー Manager, Monolithic Refractories Technology Dept., Refractories Manufacturing Div..
*** 関西・瀬戸内支店 和歌山営業所 Wakayama Office Sales Div., Kansai Setouchi Branch.
**** 日本製鉄株式会社 設備・保全技術センター無機材料技術部 無機材料技術室 主幹研究員 Senior Researcher, Refractory Technology Dept., Refractory Ceramics Div., Plant Engineering and Facility Management Center, NIPPON STEEL CORPORATION.
***** 日本製鉄株式会社 関西製鉄所和歌山地区製鋼部 炉材室長 Senior Manager, Head of Dept., Refractory Technology Dept., Steel Making Div., Kansai Works Wakayama Area, NIPPON STEEL CORPORATION.

Table 1 Composition of conventional castable* for lance
(/ mass%)

| Al ₂ O ₃ | MgO | Others |
|--------------------------------|-----|--------|
| 89 | 8 | 3 |

* Composition without stainless steel fibers

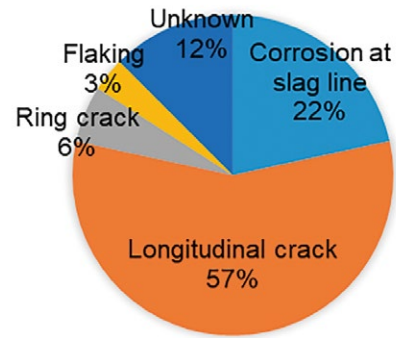


Fig. 1 Breakdown percentage of reason for exchange of the LT lance in years of 2017 and 2018.

2・2 LT ランスの実機使用後品調査結果

使用後品において、亀裂は吐出口および下端部を中心に発生していることが図 2 に示す外観写真から判る。一部のランスでは下端部に発生した亀裂を起点に先端部（吐出口付近）の剥落が発生している。使用後品を部分的に解体した際のランス内部の状態を図 3 に示しており、発生した縦亀裂の一部は芯金まで進展し、耐火物の剥離を起こすことによって、露出・溶融し、処理不可にいたる危険性を示唆している。

2・2 Results of investigating LT lance after use in actual operation

The appearance photograph after use in Fig. 2 apparently showed that the cracks occurred mainly at the vicinity of discharging ports and the tip of the lance. In some cases, tip flaking (near the ports) occurred due to the extension of crack at the vicinity of the top. Fig. 3 shows the damages of the lance after use in more detail. A part of the longitudinal cracks reached to the core steel tube, resulting in shut-down of the treatment due to risk of meltdown of the tube by peeling off the refractories covered the tube.




| | Conventional | | |
|----------------------|-------------------------------------------------------------------------------------|-------------------------------------------------------------------------------------|---------------------------------------------------------------------------------------|
| | 20 | 8 | 10 |
| Life / ch | 20 | 8 | 10 |
| Immersion time / min | 123.0 | 51.0 | 77.0 |
| Exchange reason | Longitudinal crack tip flaking | Longitudinal crack | Tip flaking |
| Appearance |  |  |  |

Fig. 2 Appearance of typical damages observed in the LT lances after use.

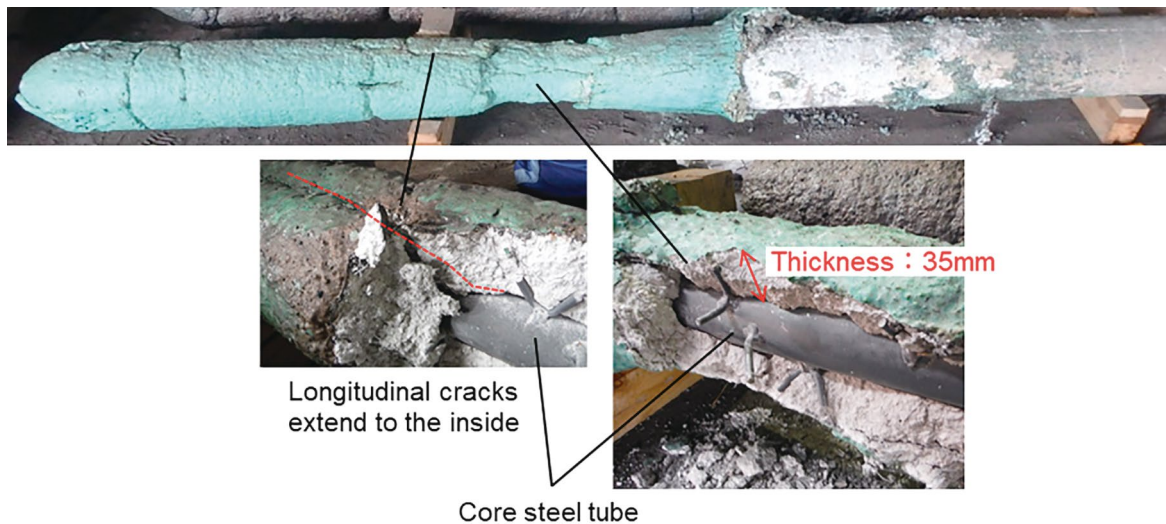


Fig. 3 Detail of the damages appeared in the LT lance after use.

3 耐火物材質の開発方針

ランス浸漬時における耐火物の表面剥離(押し割れ)を改善するため、耐火物の膨張量低減を指向した。具体的な手法としては、マグネシア量の低減によるスピネル膨張の抑制を検討した。

加えて、耐火物の緻密・高強度化によるランスの剛性向上を指向した。図4に示しているようにランスに3つの吐出口があることから、ガス吹込み時に回転モーメントが発生(但し、3つの吐出口からのガス吐出量が常時一定であれば回転モーメントは発生しないが、吐出口周辺の耐火物の損耗状況の違いにより、各吐

3 Guidelines for development of castable

In order to decrease the peeling (press cracking) of the refractories covering the steel tube during immersion, we aimed to reduce the thermal expansion of the refractories at higher temperature corresponding to that of the molten steel. As a concrete technique, the control of the high expansion spinel component was examined by decreasing magnesia from the composition of the refractories.

In addition, by densifying and strengthening the refractories covering the tubes, we have also aimed to improve the total rigidity of the lance. The LT lance was installed to the ladle with vertical configuration as shown in Fig. 4, where the one end of the lance was fixed to a

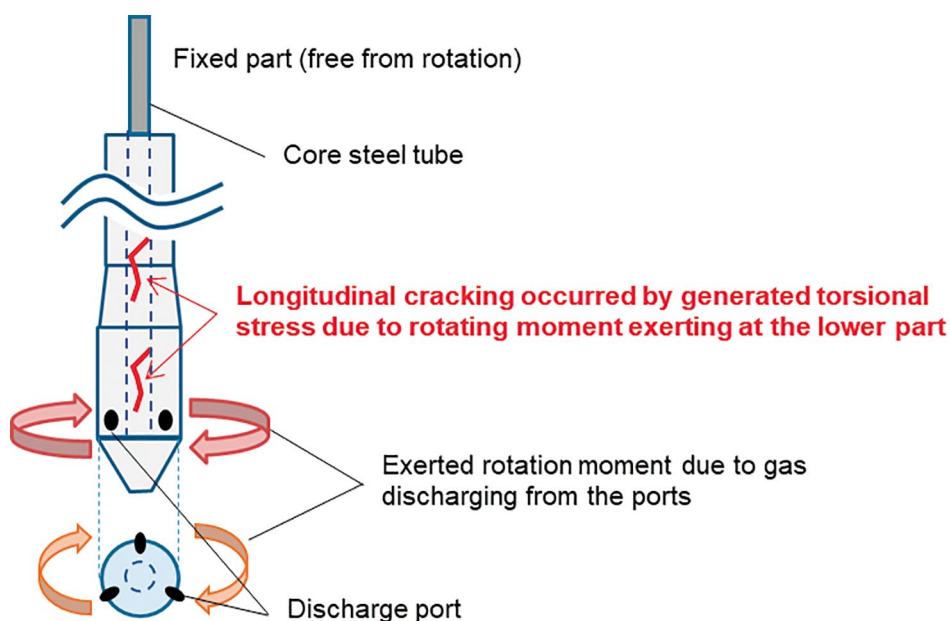


Fig. 4 Possible mechanism for occurrence of longitudinal cracking in the refractories of the LT lance.

出口よりのガス吐出量に変動が生じると推定している) し、非浸漬部のランス根元部分は固定されているため、ねじれ応力が発生する。このねじれ応力に対して、ランスの剛性(耐火物の強度)が劣っていれば、縦亀裂が発生し易くなると考えられる。図4にはこのようなねじれ応力による縦亀裂発生の推定メカニズムについて記載している。耐火物の緻密・高強度化の具体的な手法としては、分散剤種の変更による低水分化を検討した。

4 実験

4.1 実験I / 物性評価

4.1.1 供試材料

表2に供試材料の配合原料とそれらの粒径と配合量の目安、分散剤種の違い、そして添加水分量を示している。材料Aは従来から使用されているものであり、材料B及びCが新たに開発したもので、材料Aと異なる分散剤を用いており、それにより添加水分量を5.8から4.5mass%に低減している。また、材料Cは材料Aからマグネシア量を0.5a mass%低減させ、同粒度のアルミナを増量したものである。各サンプルについて110℃乾燥後と1000、1200そして1500℃の各温度で3h焼成後の状態における残存線膨張変化、曲げ強さ、圧縮強さ及び見掛け気孔率を評価した。

beam of the upper structure of the ladle and the other end was immersed to blow gas into the molten steel with three ports perforated in the side wall of the lance slightly upper position from the tip end. Since the lance has three ports for discharging gas, a rotational moment is generated during blowing the gas. (Although the moment does not generate when the gas blow rate from the three ports is always constant, the gas blow rate varies in the port by port with difference in the state of damaging the refractories around the port.) In the configuration described above, the rotational moment exerted at free end generates a torsional stress in the lance. If the rigidity of the lance (the strength of the refractories) is lower than the torsional stress, the longitudinal cracking of the refractories covering the steel tube will be induced. The corrosion resistance of the slag line part could be improved by densifying and strengthening of the refractories with the technique of the lowering water content in the castable by changing of the dispersant type.

4 Materials and experimental procedure

4.1 Experimental I / Physical property

4.1.1 Test materials

Table 2 shows raw material particle size, composition and required water content for the castable refractories sample of the materials A, B and C, respectively. The A is a conventional material, and the B and C are newly developed materials. For the B and C, the dispersant type was changed from that for the A. By changing the type of dispersant, the required water content for mixing castables of the B and C could be reduced from the A with 5.8mass% to 4.5mass%. The amount of magnesia in the B by 0.5a mass% from that in the A, and increased the same amount of alumina with same particle size. The permanent linear change, modulus of rupture, compressive strength and apparent porosity of each sample were measured after drying at 110℃ or firing at 1000℃/1200℃/1500℃ for 3h.

Table 2 Raw material particle size, composition and required water content of the castable refractories sample

| Sample | | | (/ mass%) | | |
|------------------------------------------|----------|--------------|--------------|------------|------------|
| | | | Material A | Material B | Material C |
| Ingredient / particle size (/ mm) | | | Conventional | Developed | |
| Type of dispersant | | | α | β | |
| Al ₂ O ₃ / +1mm | | raw material | 45 | | |
| Al ₂ O ₃ / 0.1~1mm | | | 27.5 | | |
| Al ₂ O ₃ | / -0.1mm | matrix | b | | b+0.5a |
| MgO | | | a | | 0.5a |
| *CAC | | | c | | |
| SiO ₂ | | | d | | |
| Others | | | e | | |
| Water | | | 5.8 | 4.5 | |

*CAC : Calcium aluminate cement

(a,b,c,d,e : constants)

4・1・2 実験結果

図5に各熱処理条件ごとの残存線変化率(a), 見掛け気孔率(b), 曲げ強さ(c)そして圧縮強さ(d)の評価結果を示している。図に見られるように材料Cはマグネシア量の低減により, スピネル生成量を低減でき, 狙い通りに1200℃と1500℃焼成材の残存膨張量を抑制できた。各熱処理条件とも材料B及びCは曲げ及び圧縮強さが向上しており, 特に1000℃と1200℃焼成材の強度向上が顕著であった。さらに, 材料B及びCの低水分化による見掛け気孔率の低下も見られ, 特に材料Cでは焼成温度 $\geq 1200^{\circ}\text{C}$ でのスピネル生成量の低減による結果として, 残存膨張量の抑制効果でさらなる緻密化(見掛け気孔率の低減)が達成された。材料Cにおいて残存膨張量の抑制, 緻密化および高強度化が達成できた。そこで, 次に実機使用時の亀裂抑制効果を確認するために, 耐熱スポーリング性の評価を実施した。

4・1・2 Results

Figure 5 shows the results of measurement in the linear expansion (a), apparent porosity (b), modulus of rupture (c), and compressive strength (d) for all the samples with each heat treatment condition. As seen in the figure, the reduction in the spinel formation due to decreasing addition of magnesia succeeded in suppressing permanent linear change of the C fired both at 1200 and 1500°C. The strengths of developed materials fired in each temperature were higher than those of the A. Especially, the strength increase was remarkable in the materials fired at both 1000 and 1200°C. The developed materials with fired at each temperature had low apparent porosity due to their lowered water content in the green state. Especially, in the C densification was achieved by not only reduction in water content but suppression in permanent linear change by reducing the formation of spinel at firing temperatures higher than 1200°C. As the results, the higher strength was also achieved in the C, finally. Then, we try to check the ability of the developed materials to suppress cracking in the actual use though the thermal spalling test.

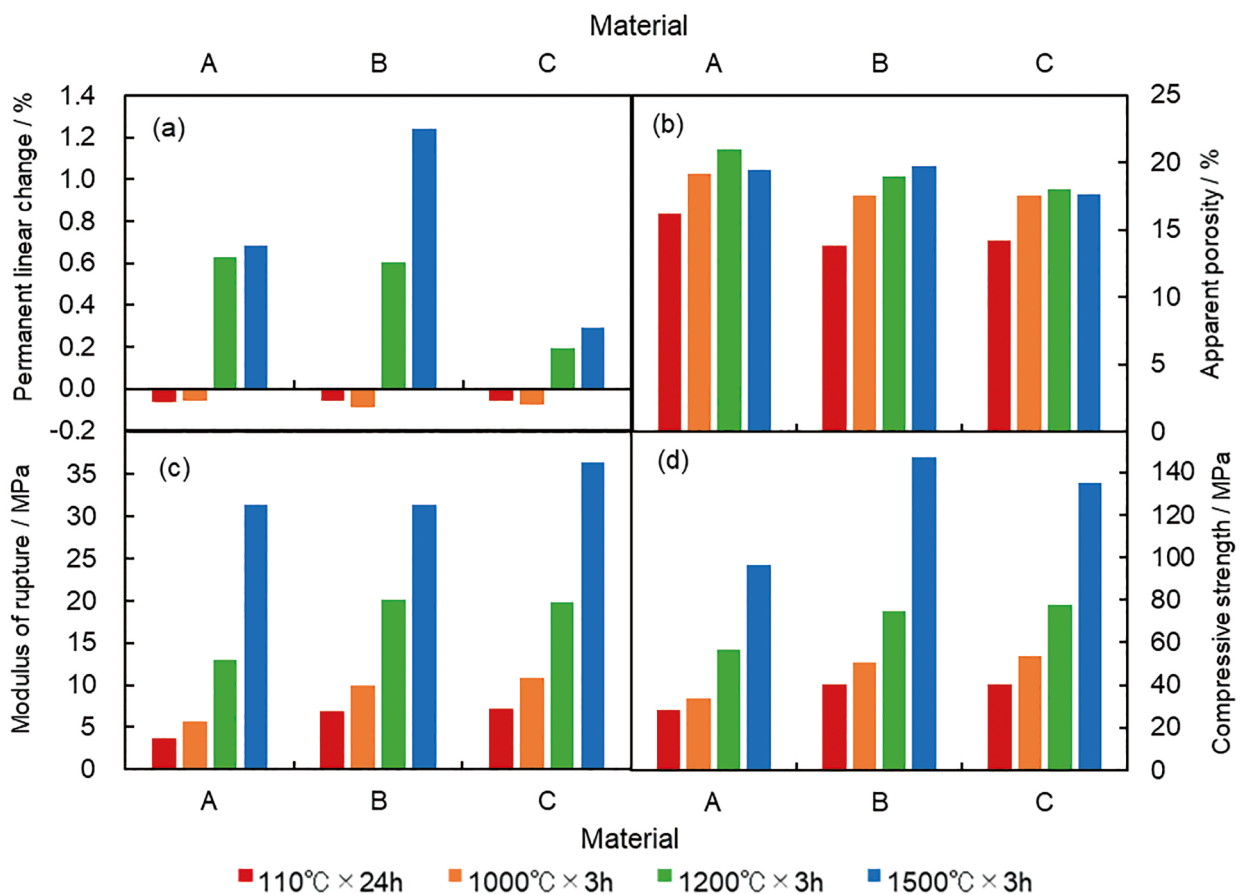


Fig. 5 Measured properties of (a) permanent linear change, (b) apparent porosity, (c) modulus of rupture and (d) compressive strength for materials A, B and C with various heat treatment conditions showing below the figure.

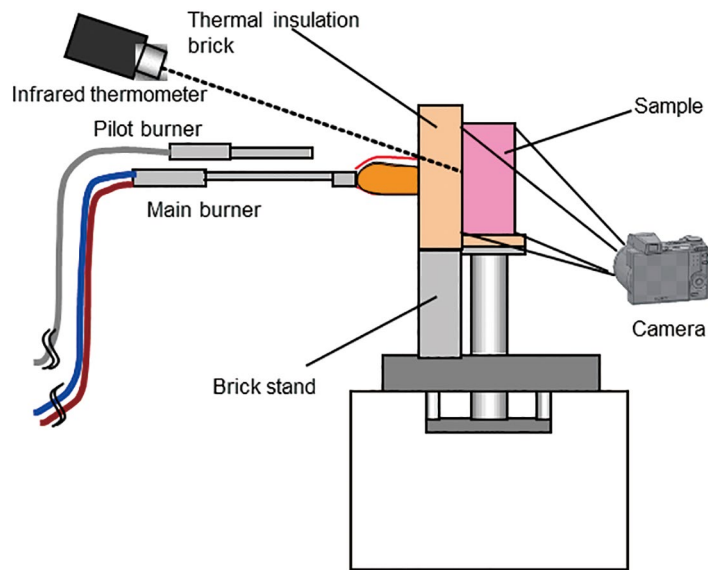


Fig. 6 Scheme of experimental set-up for thermal spalling test equipment.

4・2 実験Ⅱ / 耐熱スポーリング性の評価

4・2・1 実験手法

試験装置及び方法を模式的に図 6 に示している¹⁾。加熱は急加熱できるプロパン-酸素バーナーで行い、遮熱煉瓦を加熱面側の外周に配置し、側面への炎の回り込みを防いだ。片面加熱により高温部から低温部の領域となる試料側面の撮影は、試料が冷えないように、撮影時にもみ移動する断熱材を設置して実施し、また温度は非接触式の赤外温度計により測定した。ひずみ量はこの面のデジタルカメラによる撮像データをデジタル画像相関法により処理し、変形前後の変位と初期長さから算出した²⁾。亀裂発生時にはひずみ量が増大し、亀裂幅、長さの定量的評価が可能である。

4・2・2 供試材質と評価条件

評価材料は材料 A (従来材) と C (開発材) とし、それぞれにステンレス鋼ファイバーを f mass% 添加したものを基本組成とした。また、ステンレス鋼ファイバーの添加量の影響を調べるため、C において添加量を $0 \sim f$ mass% の範囲で変化して試験した。表 3 に全試料のファイバー添加量をまとめて示している。試料は 110°C で 24h 乾燥後、 1000°C で 3h 焼成した。耐熱スポーリング試験片の形状は $230 \times 114 \times 65\text{mm}$ で、図 6 に示す加熱面は $230 \times 65\text{mm}$ 、撮像面は $230 \times 114\text{mm}$ とした。

4・2 Experimental II / Thermal spalling test

4・2・1 Experimental procedure

Figure 6 shows a schematic image of the equipment for thermal spalling test¹⁾. In the test, one side (heating surface) of the sample with prismatic shape was quickly heated by a propane-oxygen gas burner. The thermal insulation brick with longer side of the heating side of the sample was arranged on the front of the heating side to prevent the burner flame from going around to the other sides. In one of the side surface other than the front heating surface, there is a temperature gradient from high in the front heating surface to low in back side surface, originating thermal stress to give strain to the sample. The photographs were taken in such side surface with certain interval. The side surface is covered by the heat insulating material which is removed just at the timing of the photographing to prevent the sample cooled from unfavorable direction. Then, amount of strain was calculated from the displacement before and after deformation due to thermal stress and the initial length by processing the image data of the sample using the digital image correlation method²⁾. It is possible to evaluate crack width and length quantitatively in the method, since increase in the calculated strain is reflected in initiation to propagation of the crack.

4・2・2 Test materials and condition

We evaluated the material A (conventional) and material C (developed). The A was evaluated by adding f mass% of stainless steel fiber. In order to investigate the effect of the amount of stainless steel fibers on the heat-resistant spalling properties, the C was evaluated by adding 0 to f mass% of the fibers as shown in Table 3. The sample was $230 \times 114 \times 65\text{mm}$ prismatic shape, with heat treatments of drying at 110°C for 24h, and then firing at

試験は昇温速度 200°C/min で 1600°C まで加熱し 10min 保持, その後 10min 冷却するサイクルを 3 回繰り返した。その際に計測した温度変化の一例を図 7 に示す。試験中の撮像間隔は 67s とし, 加熱開始から, 昇温中である 201s 後と 402s 後, 1 回目の 1600°C × 10min 加熱保持後である 871s 後, 冷却し 2 回目の保持後である 2479s 後, さらに 3 回目の保持後である 4079s 後のひずみ分布を測定し, 図 8 に全試料の各時間経過後のひずみ分布図を示している。なお, これらのひずみ分布の出力時期を図 7 に赤四角印として示している。

1000°C for 3h. The heating front surface of the thermal spalling test was 230 × 65mm, and the side surface photographed by a digital camera was 230 × 114mm. An example of the temperature change given to the sample is shown in Fig. 7 where the temperature was raised to 1600°C at the heating rate of 200°C/min, kept for 10min, and then cooled for 10min. The thermal cycle was repeated three times in the test. The strain distribution kept count at the timings of 201s and 402s after the start of heating, 871s after the first holding at 1600°C for 10min, 2479s after the second holding at 1600°C for 10min, and 4079s after the third holding at 1600°C for 10min, respectively, with the photographing interval of 67s. Fig. 8 shows the strain distributions counted at each timing shown also in Fig. 7 for all the samples tested.

Table 3 Test materials with addition of stainless steel fiber

| Matrix | Material A | Material C | | | | |
|-------------------------------|--------------|------------|-------|------|-------|---|
| | Conventional | Developed | | | | |
| Stainless steel fiber / mass% | f | 0 | 0.25f | 0.5f | 0.75f | f |

f : constant

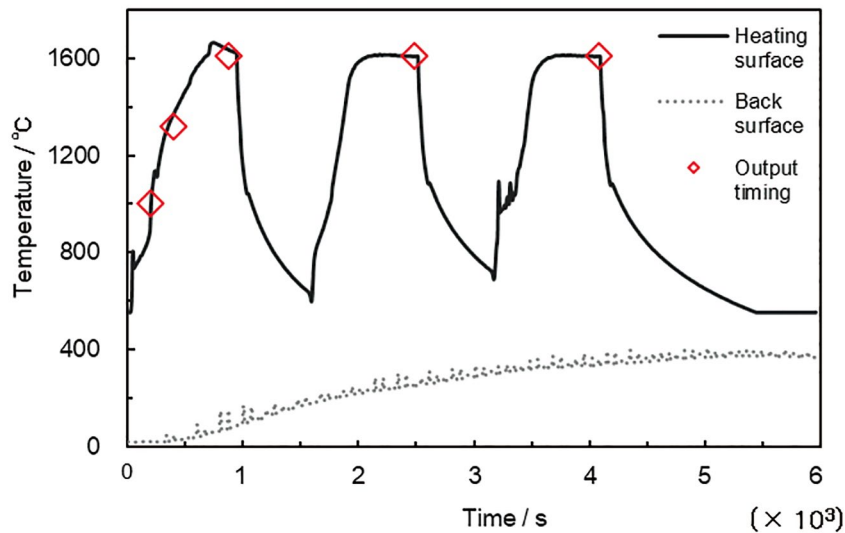


Fig. 7 Heating schedule of test samples and measured temperature at both heating and back surfaces.

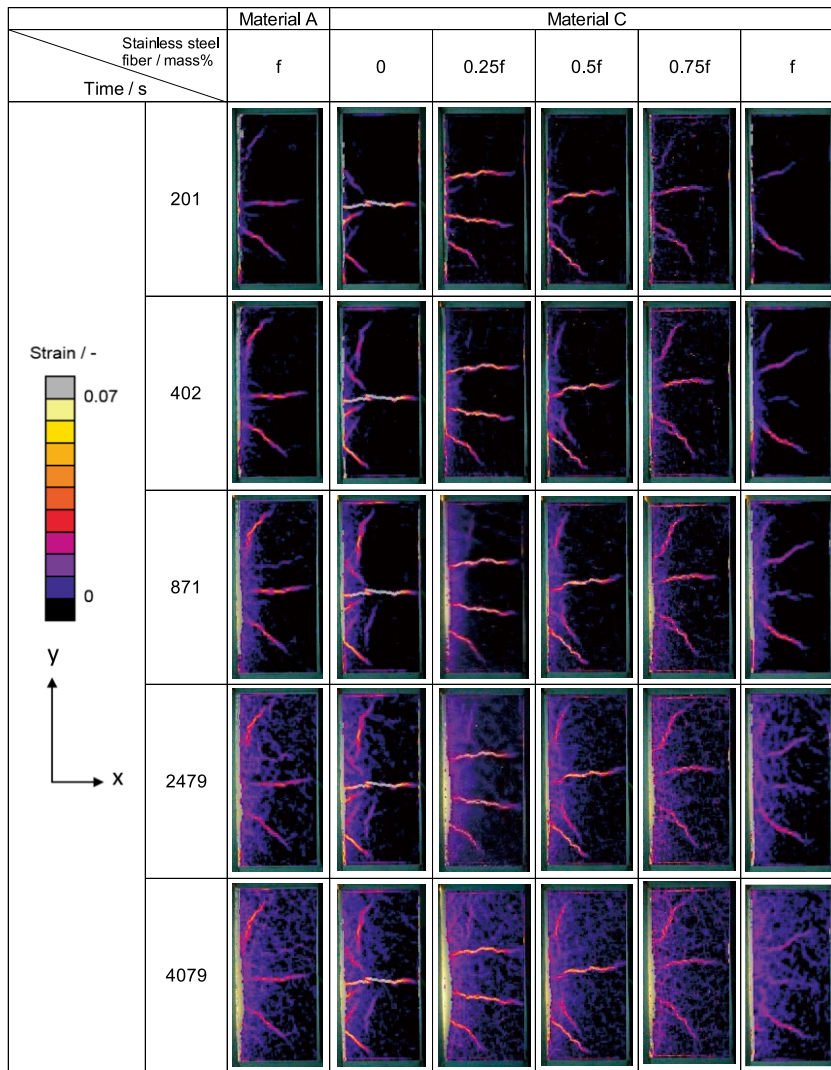


Fig. 8 Shift of strain distribution with time on the thermal spalling test for all the samples tested.

4・2・3 実験結果及び考察

材料の耐熱スポーリング性を定量的に評価する亀裂指数は図8に示すひずみ分布図から全方向(x方向とy方向)のひずみ量を算出し、以下の式のように定義した。

$$\text{亀裂指数} = (\text{全評価点の2\%以上のひずみ量の総和}) / (\text{全評価点の数})$$

図9には図7に示した各出力時期における供試全サンプルの亀裂指数の算出結果を示している。ステンレス鋼ファイバーをf mass%添加した材料A(従来材)と材料C(開発材)を比較すると、材料Cは各出力時期とも亀裂指数が小さく、耐熱スポーリング性に対して優位である事が分かる。4079s時点(3回目の

4・2・3 Results and discussion

The crack index, as one of the measures of the thermal spalling resistance, was defined as the following equation by calculating the amount of strain in all directions (x- and y-directions) in the strain distribution (Fig. 8).

$$\text{Crack index} = (\text{Total sum of strains higher than 2\% at the whole detecting positions}) / (\text{Total number of the detecting positions})$$

Figure 9 shows the calculated crack index at the output timing shown in the Fig. 7 for all the samples tested. Comparing the A (conventional) and the C (developed) both with f mass% stainless steel fiber, the C had smaller crack index at all the timings detected, showing apparently superior thermal spalling resistance to the A. Fig. 10 shows the relationship between the crack index at 4079s (after the third holding at 1600°C for 10min) and the amount of

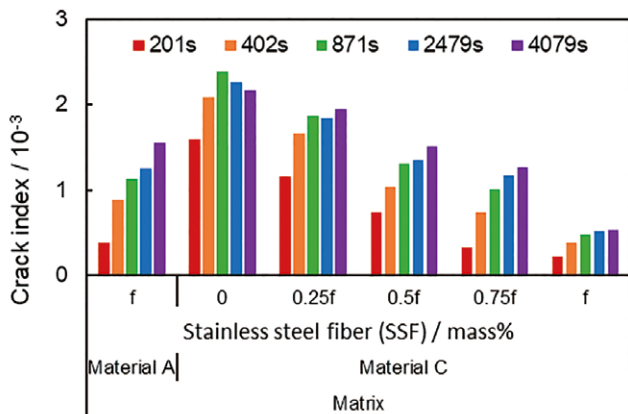


Fig. 9 Comparison of crack index calculated at the timings shown in the figure for all the samples tested.

1600°C × 10min 保持後) での亀裂指数とステンレス鋼ファイバーの添加量の関係を図 10 に示す。材料 C に関して、ステンレス鋼ファイバーの添加量と亀裂指数には線形性の強い相関がみられ、ランス耐火物へのステンレス鋼ファイバー添加の有効性が確認できた。

次に、耐熱スポーリング性の評価で算出された亀裂指数と、各種耐熱衝撃性を表す指標³⁾である熱衝撃破壊抵抗 R 、熱衝撃損傷抵抗 R''' 、クラック安定係数 R_{st} および破壊エネルギー γ^4 との相関を調査した。各種耐熱衝撃性評価式を以下に示す。

$$R = \frac{S(1-\nu)}{E\alpha} \quad R''' = \frac{E\gamma}{S^2(1-\nu)} \quad R_{st} = \left(\frac{\gamma(1-\nu^2)}{E\alpha^2} \right)^{\frac{1}{2}}$$

ここで、 S : 常温曲げ強さ、 E : 圧縮静弾性率、 γ : 破壊エネルギー(切欠き梁の三点曲げ試験より測定⁵⁾)、 ν : ポアソン比、 α : 熱膨張係数 尚、上記 S , E , γ の値は 1000°C × 3h 焼成後のサンプルでの測定値を用いた。

4079s 時点 (3 回目の 1600°C × 10min 保持後) での亀裂指数、各種耐熱衝撃性を表す指標と破壊エネルギーとの関係を図 11 に示す。

亀裂指数と R に相関は見られなかったが、 R''' は強い相関がみられた。また、亀裂指数と破壊エネルギー γ にも強い相関がみられた。 R''' に強い相関がみられたのは、 R''' 式を構成する破壊エネルギー γ によるものである。破壊エネルギー γ を増大させる事が亀

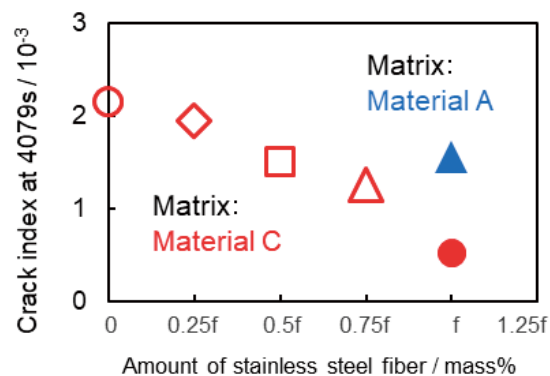


Fig. 10 Effect of stainless steel fiber addition on the crack index at 4079s.

stainless steel fibers added. Since there was a strong correlation between the crack index and the amount of the stainless steel fiber for the C, the usefulness of the stainless steel fiber addition to the refractories used for the lance was able to be confirmed.

We investigated the correlations between the calculated crack index determined by the thermal spalling test and various indices representing thermal shock resistance³⁾, which are thermal shock fracture resistance R , thermal shock damage resistance R''' and thermal shock fracture resistance R_{st} , as well as, fracture energy γ^4 .

The equation expressing them are shown below;

where, S : modulus of rupture, E : modulus of elasticity, γ : fracture energy (measured by three-point bending test of notched beam⁵⁾), ν : poisson's ratio, α : thermal expansion coefficient. (Values for S , E and γ were measured in sample fired at 1000°C for 3 h).

Figure 11 (a)-(d) shows the relationships of the calculated crack index at 4079s (after the third holding at 1600°C for 10min) with the fracture energy and the three indices representing thermal shock resistance. Although there was no strong correlation of the R with the crack index (a), the other two indices for thermal shock resistance R''' and R_{st} correlated strongly with the crack index (b, c). The fracture energy γ has also strong correlation with the crack index (d). The strong correlations of the R''' and the R_{st} with the crack index depended on the fracture energy

裂抑制を図る上で非常に重要である事が分かる。亀裂指数と R_{st} に関して、マトリックスが材料 C の場合で比較すると強い相関がみられた。ステンレス鋼ファイバーの添加が R_{st} の向上に強く作用する事が分かった。

γ which constitutes both equations for the R''' and the R_{st} . Therefore, controlling of the fracture energy γ is important for suppressing the crack. It was also proven in the C that the increase in amount of the stainless steel fibers addition was quite effective to improve the R''' , R_{st} , and γ .

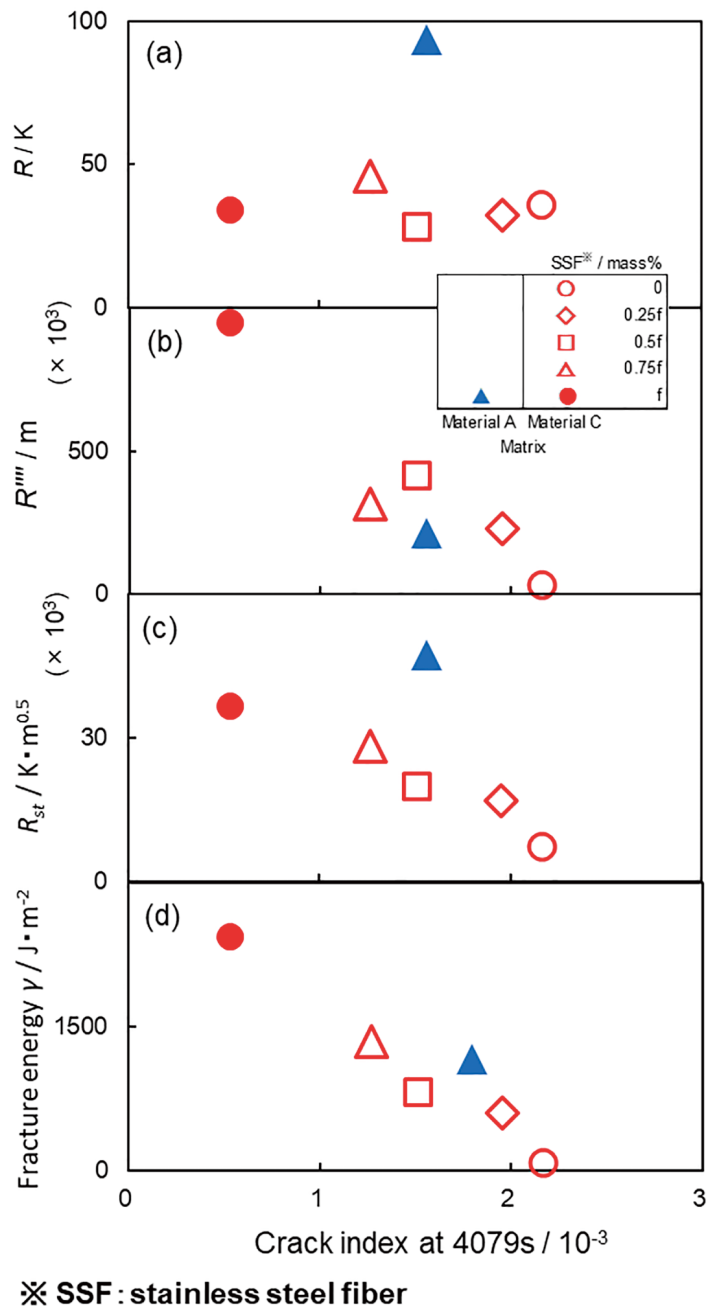


Fig. 11 Correlation of the crack index at 4079s with various parameters of (a) R , (b) R''' , (c) R_{st} and (d) fracture energy.

5 実機試験

ラボ試験で亀裂抑制に有効であったステンレス鋼ファイバーを f mass% 添加した材料 C について、実機でご使用いただいた。

5・1 初回試験品の使用後外観

2019/12～2020/1にかけて、開発したランスを実機にてご使用いただき、耐用16ch、累積処理時間120minと良好な結果を得た（従来品：11.1ch、88min）。

使用後品の写真を図12に示す。従来品で発生していた深い大きな縦亀裂やリング亀裂は発生しなかった。交換理由はスラグライン部の溶損であった。

使用後品を解体した際の内部写真を図13に示す。スラグラインとメタルライン部の稼働面側（外側）は受熱により、ステンレス鋼ファイバーは一部酸化していたが、非稼働面側（内側）では酸化されずに存在していた。非浸漬部のステンレス鋼ファイバーは、どの部位も健全に存在していた。また、すべての部位においてステンレス鋼ファイバーは分散して存在していた事が確認された。

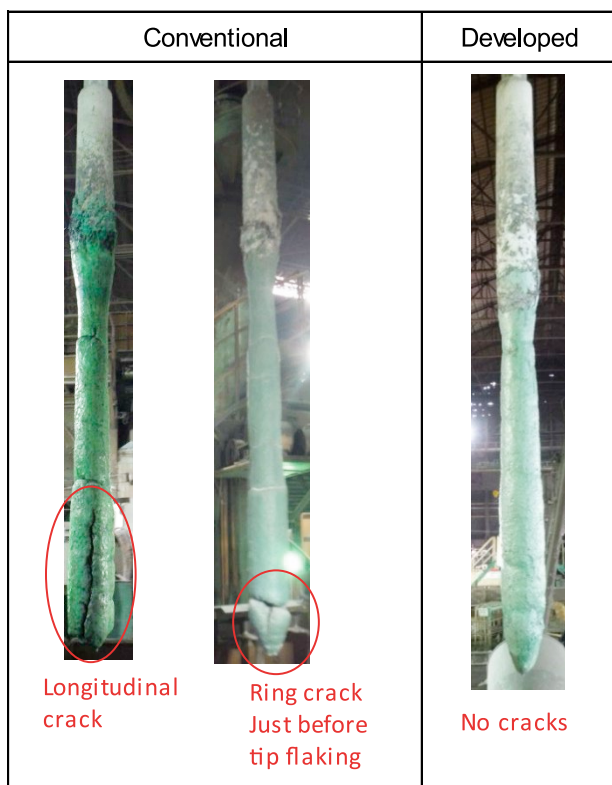


Fig. 12 Views of conventional and developed LT lances after use in actual operation.

5 Test in actual operation

The material C with f mass% stainless steel fibers, exhibited a high performance in the laboratory thermal shock test with the lower crack index, was used in actual operation.

5・1 Initial test results of developed LT lance

From December, 2019 to January, 2020, the developed LT lance was used in actual operation, and marked an improved performance in both service life and cumulative immersion time of 16ch and 120min (conventional by 11.1ch and 88min), respectively.

Figure 12 shows views of the LT lance after use. Deep and large longitudinal and ring cracks occurred frequently in the conventional LT lance were not observed. The reason for determining the exchange of the lance changed from cracking to the corrosion of the slag line.

Figure 13 shows the magnified views of the damages in the lance after use. The working surface (outside) of the slag and metal lines were damaged by the heat with oxidizing partially the stainless steel fibers, although, they were not oxidized on the non-working side (inside). In non-immersed part of the lance, refractories remained in a sound state with confirming also uniform dispersion of the stainless steel fiber in all positions.

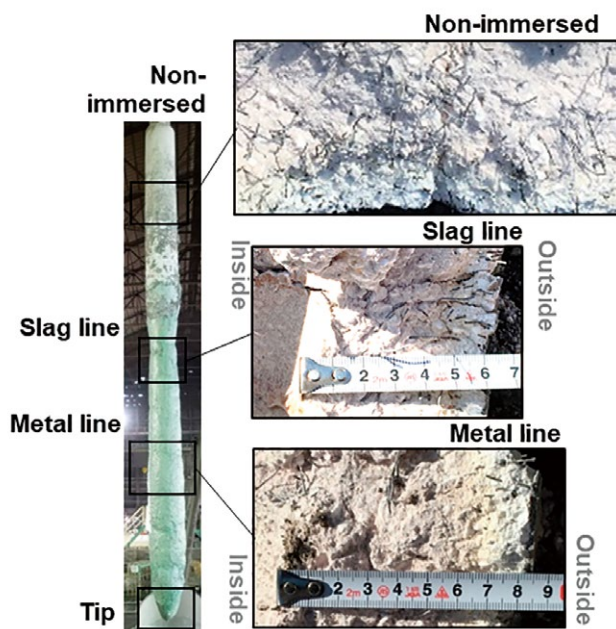


Fig. 13 Magnified view of each damaged part of the developed LT lance shown in Fig. 12 after dismantling.

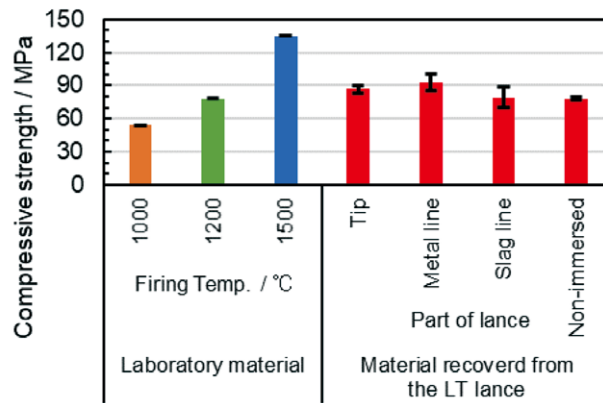


Fig. 14 Evaluation of compressive strength of newly developed material for both laboratory and recovered them after using as the LT lance.

使用後品の各部位における圧縮強さを図 14 に示す。ラボ試験データと比較した結果、どの部位も十分な強度を有しており、施工体の健全性が確認できた。

5・2 改善品の耐用調査まとめ

2019/12～2020/5の期間(N数=26)における開発材の実機での耐用結果を図 15 に、交換理由を図 16 に示す。継続使用いただいたが、開発材の耐用は良好であり、従来材に比べて、平均耐用は 11.1ch から 18.0ch、平均累積処理時間は 88min から 121min へと大幅に向上した。縦亀裂を起因とするランス交換は発生しておらず、スラグライン部の溶損が交換理由の 90% 以上を占めた。

開発材の耐用状況が良好であったことから、工程化される事となった。

Figure 14 shows the comparison of the compressive strength of each part of the lance after use with laboratory test data for materials fired at 1000 to 1500°C. Even in after use, all the parts had sufficient strength, and soundness of the construction body was able to be confirmed.

5・2 Results of developed LT lance

Figure 15 compares the durability of the developed LT lance in the actual operation in the period of December, 2019 to May, 2020 (N = 26) with that of conventional one. The reason for the exchange in the case of developed lance are shown in Fig. 16. It has an improved durability with the average life from 11.1 to 18.0ch, and the average cumulative immersion time from 88 to 121min compared to the conventional one. The reason for exchanging changed from the lance longitudinal cracking to corrosion of slag line with sharing 90%. Since the developed LT lance had excellent durability, it became to be used steadily in the actual operation.

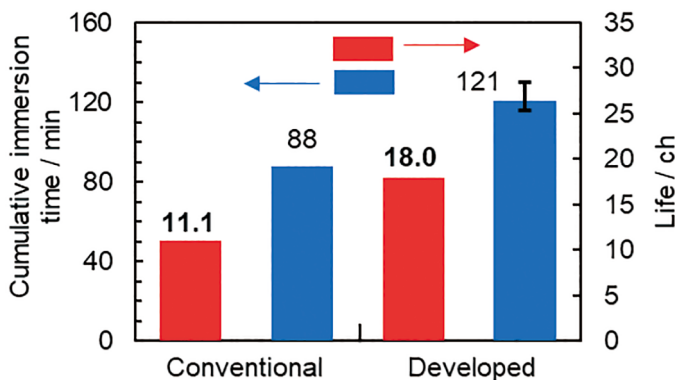


Fig. 15 Comparison of cumulative immersion time and life for the conventional and the developed LT lance.

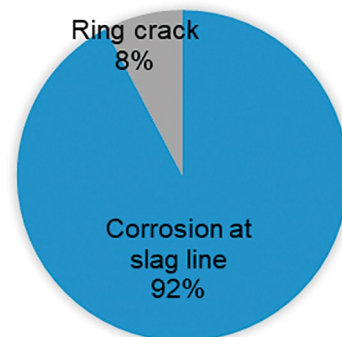


Fig. 16 Reason for exchange of the newly developed LT lance.

6 結言

日本製鉄(株)関西製鉄所和歌山地区ステンレス製鋼工場 LT ランスに関して、下端部の亀裂発生抑制に取り組んだ結果、

- (1) 従来材に対して、マグネシア量の低減によるスピネル膨張の抑制と、分散剤種の変更による低水分緻密化を図った材料を開発した。
- (2) 開発材は $\geq 1200^{\circ}\text{C}$ で残存膨張量の抑制、高強度化および見掛け気孔率の低減ができた。
- (3) 従来材に比べて、開発材は耐熱スポーリング性も良好な結果が得られ、今回実施した熱スポーリング試験結果から算出した亀裂指数は、熱衝撃損傷抵抗 R''' および破壊エネルギー γ に強い相関があった。
- (4) 開発材を適用したランスを実機で使用した結果、従来材に比べて、平均耐用は 11.1ch から 18.0ch、平均累積処理時間は 88min から 121min へと大幅に向上した。課題であった下部の亀裂発生も抑制され、損耗要因はスラグライン部の溶損に変わった。

上記の通り、開発材の耐用は良好であった為、開発材は工程化される事となった。

文 献

- 1) 辻陽一，神尾英俊，細木亮太，後藤潔，森川勝美：第 6 回鉄鋼用耐火物専門委員会報告集，耐火物技術協会 pp.151-157 (2018)。
- 2) Hidetoshi Kamio: Proceedings of Unitecr 2011 2-B1-2.
- 3) 耐火物技術協会編：耐火物手帳改訂 12 版，pp. 101-102 (2015)。
- 4) 耐火物技術協会編：耐火物手帳改訂 12 版，pp. 86 (2015)。
- 5) 耐火物技術協会編：耐火物手帳改訂 12 版，pp. 102 (2015)。

本論文は以下の報文に加筆・再構成して転載したものである。

笹谷他：第 9 回鉄鋼用耐火物研究会講演会報告集，耐火物技術協会 (2021) pp.78-87.

6 Conclusions

As the result of efforts on decreasing the occurrence of the crack at the vicinity of tip in the LT lance, using in the stainless steel plant of NIPPON STEEL CORPORATION Kansai Works Wakayama Area, the following improvement were achieved.

- (1) New material of refractories for the LT lance was developed with decreased spinel expansion by reducing the magnesia content, and densification with low water content by changing the dispersant.
- (2) The developed material had the lower permanent expansion change, the higher strength, and the lower apparent porosity when fired at the temperatures higher than 1200°C compared to the conventional one.
- (3) The thermal spalling properties of the developed material was superior to the conventional one. The crack index obtained by the thermal spalling test was strongly correlated with the thermal shock damage resistance R''' and the fracture energy γ .
- (4) The durability of the LT lance with developed material in actual operation, was increased significantly both in the average life and cumulative immersion time from 11.1ch and 88min to 18.0ch and 121min, respectively. Since the occurrence of cracking at the vicinity of top decreased in the lance, the exchange reason changed to the corrosion of slag line for the LT lance with the developed materials.

As described above, since the developed LT lance exhibited a high durability, it became to be used steadily in the actual operation.

References

- 1) Yoichi Tsuji, Hidetoshi Kamio, Ryota Hosogi, Kiyoshi Goto and Katsumi Morikawa: Proceedings of the 6th Annual Meeting of Technical Committee of Refractories for the Iron and Steel, Technical Association of Refractories, Japan (2018) pp.151-157.
- 2) Hidetoshi Kamio: Proceedings of UNITECR 2011, 2-B1-2 (2011).
- 3) The Technical Association of Refractories of Japan (TARJ) ed.: Refractories Handbook, Revised edition 12 (2015) pp.101-102.
- 4) The Technical Association of Refractories of Japan (TARJ) ed.: Refractories Handbook, Revised edition 12 (2015) p.86.
- 5) The Technical Association of Refractories of Japan (TARJ) ed.: Refractories Handbook, Revised edition 12 (2015) p.102.

This paper is reprinted with some additions and reconstructions to the following paper:

Sasatani et al.: Proceedings of the 9th Symposium on Refractories for Iron and Steel, Technical Association of Refractories, Japan (2021) pp.78-87.